JTTEE5 11:226-232




# Splat Morphology and Microstructure of Plasma Sprayed Cast Iron With Different Preheat Substrate Temperatures

*M.F. Morks, Y. Tsunekawa, M. Okumiya, and M.A. Shoeib*

*(Submitted 9 November 2000; in revised form 9 March 2001)*

**A cast iron coating is a prime candidate for the surface modification of aluminum alloys for antiwear applications because cast iron is inexpensive and exhibits superior wear resistance arising from the self-lubricating properties of graphite. In the present study, fundamental aspects of a plasma sprayed cast iron coating on an aluminum alloy substrate, including (1) the effects of preheat substrate temperature on the splat morphology, (2) the formation of a reaction layer and pores, and (3) the splat microstructure, were investigated in low-pressure plasma spraying. With an increasing substrate temperature, the splat morphology changes from a splash type to a disk and star shape. Deformed substrate ridges, mainly resulting from the slight surface melting, are recognized adjacent to the splat periphery at high substrate temperatures. The flattening ratio of disk splats decreases with substrate temperature because the ridges act as an obstacle for splat expansion. A reaction layer composed of iron, aluminum, and oxygen is ready to form at high substrate temperatures, which, along with the deformed ridges, improves the adhesive strength of splats. However, the pores appear at the splat interface at low substrate temperatures, which hinder the formation of a reaction layer. The amount of graphitized carbon increases in cast iron splats with an increase in substrate temperature.**

**Keywords** aluminum alloy substrate, cast iron, deformed substrate ridge, pore, reaction layer, splat morphology

## 1. Introduction

To promote material substitution from ferrous materials to aluminum alloys for the purpose of weight reduction, surface modification is required to improve the poor wear resistance of aluminum alloys owing to their softness. There have been three major surface modification processes to the bores of cast aluminum alloy automotive cylinder blocks: selectively incorporated metal matrix composites,[1] electroplated nickel bores with hard particles,[2] and plasma sprayed steel coatings.[3-5] Kim et al.[3] reported that increased droplet velocity causes a greater coating/substrate adhesion in plasma spraying of steel on an aluminum alloy substrate. In contrast, sprayed coatings of iron with different aluminum contents have been examined to elucidate the oxidation in a high velocity oxyfuel process,[6] in which the oxidation occurs in the liquid state and during impact with an aluminum substrate. A thin oxide film between the splats also develops after the solidification. The oxides are composed of a mixture of $Al_2O_3$, $FeAl_2O_4$, and FeO.

Sprayed cast iron coatings are also considered a prime candidate for surface modification because cast iron is relatively inexpensive and exhibits superior wear resistance arising from the self-lubricating effect of graphite. However, sprayed cast iron coatings generally contain carbides instead of graphite.[7] The microstructure and mechanical properties of sprayed coatings are determined by (1) the flattening dynamics of molten droplets impinging on a substrate, (2) the solidification rate of resultant splats, and (3) any interfacial reactions with the underlying substrate surface.[8] Solidification of a single splat is nearly independent on the impingement of forthcoming splats. Thus, the microstructure and performance of sprayed coatings can be estimated by the flattening behavior and solidification of a single splat.[9-12]

The effect of substrate temperature on the splat morphology has been intensively studied over the last 10 years.[13-15] All of these studies showed that splash-type splats appear at low substrate temperatures and disk splats evolve at high substrate temperatures, although the transition temperature[16] on splat morphology varies for different metals and substrates. Thermal resistance at the interface, such as pores and reaction layers, plays an important role to the solidification rate of splats.[17] On the other hand, preheating a substrate generally decreases the splat solidification rate, which also affects the microstructure. Furthermore, the splat morphology at the first layer sprayed on a substrate surface markedly affects the adhesive strength of coatings.[18]

The present work studied the fundamental aspects of plasma sprayed cast iron coatings on a low melting point aluminum alloy substrate. For this purpose, the effects of preheat substrate temperature on the splat morphology, adhesion, formation of a reaction layer and pores, and microstructure were examined using a cast iron powder with a uniform size under low-pressure plasma spraying. The deformed ridge formation on a substrate during the flattening of splats and its influence on the flattening ratio are also discussed.

**M.F. Morks, Y. Tsunekawa,** and **M. Okumiya,** Toyota Technological Institute, Nagoya, Japan; and **M.A. Shoeib,** Central Metallurgical Research and Development Institute, Cairo, Egypt. Contact e-mail: tsunekawa@toyota-ti-ac.jp.

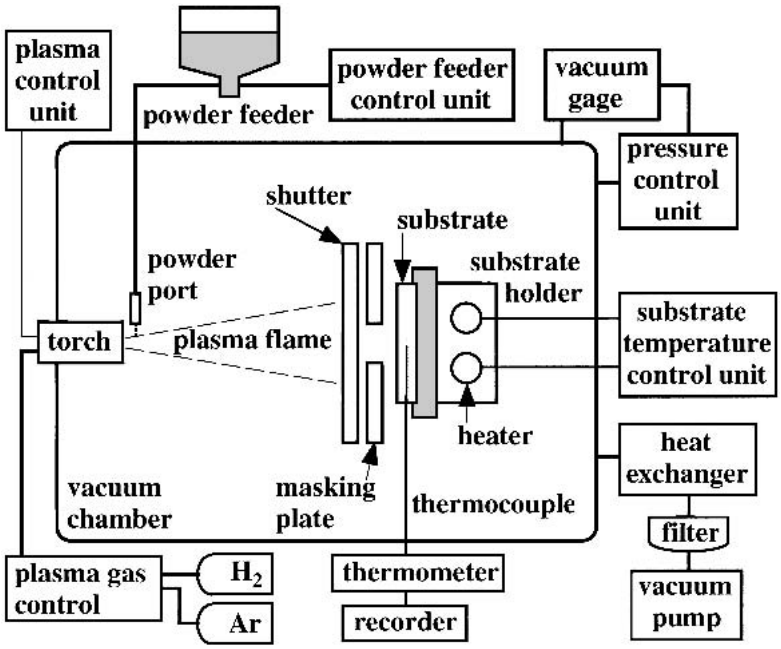


**Fig. 1** Schematic diagram of low-pressure plasma spray apparatus with a splat collection system

## 2. Experimental Procedures

A gas-atomized cast iron powder with chemical composition of Fe-3.75C-2.70Si-0.70Mn-1.18Al (all compositions in weight percent) was prepared as a spray material. The nearly spherical-shaped powder was composed of a rapidly solidified Fe-Si-C and $Fe_3C$ phase. It was sieved into a diameter range of 38-45 μm and fed into a plasma flame in low chamber pressure. The low-pressure plasma spray apparatus is described in Fig. 1 with a splat collection system. Sprayed cast iron droplets were impinged on a mirror-finished Al-Si-Cu alloy substrate, which had been achieved by buff polishing. The substrate preheating was performed by cylindrical sheath-type heaters embedded in a substrate holder and connected with a temperature control unit. Substrate temperature was continuously recorded through a sheath thermocouple inserted into the center of the substrate. The spray parameters are listed in Table 1. If a movable graphite shutter installed just before the masking plate is opened for a few seconds, a limited number of molten droplets with a relatively uniform temperature and velocity can pass through a hole in the center of the masking plate, and impinge onto a preheated substrate surface.

The splat morphology of cast iron formed upon impact was observed by scanning electron microscopy (SEM), and then the flattening ratio was calculated by measuring each splat diameter. A conductive adhesive tape mainly composed of graphite was used to peel splats from the substrate to examine the rear-view appearance, and the number of removed splats was counted to evaluate the adhesive property. To observe the microstructure, cross sections and polished top views of splats were observed by SEM after etching for 60 s using a mixed reagent of HF, $H_2O_2$, $HNO_3$, and $C_2H_5OH$. The constituent phases including graphitized carbon were identified by x-ray diffraction (XRD) with a Co-Kα radiation. Element analyses were also performed on a splat surface and cross section by electron probe microanalysis (EPMA).

**Table 1 Spray Parameters for the Splat Collection on a Preheated Substrate**

| | |
|---|---|
| Primary plasma gas | Ar: $3.92 \times 10^{-4}$ ($m^3$/s) |
| Secondary plasma gas | $H_2$: $3.92 \times 10^{-5}$ ($m^3$/s) |
| Arc current | 500 (A) |
| Arc voltage | 45 (V) |
| Powder carrier gas | Ar: $4.33 \times 10^{-5}$ ($m^3$/s) |
| Chamber pressure | 46 (kPa) |
| Spray distance | 350 (mm) |
| Spray material | Cast iron ($38 < d_P < 45$ μm) |

## 3. Results and Discussion

### 3.1 Splat Morphology of Cast Iron

Three different types of splat morphology exist: a splash type, disk, and star shape are observed for cast iron splats sprayed at different preheat substrate temperatures ($T_S$), as typically shown in Fig. 2, in which the substrate temperature greatly affects the splat morphology. Splash-type splats mainly appear at low substrate temperatures. In contrast, disk- and star-shaped splats are formed at high temperatures. Splash-type splats have a central disk surrounded by network lines, and star-shaped splats are a type of disk splat with long radial streaks. The transition behavior in splat morphology of sprayed cast iron is quantitatively described in Fig. 3 as a function of preheat substrate temperature ($T_S$). The transition temperature ($T_t$) on splat morphology, at which 50% of splash-type splats change to a disk shape,[16] is 450 K for the present plasma sprayed cast iron. The number fraction of star-shaped splats gradually increases

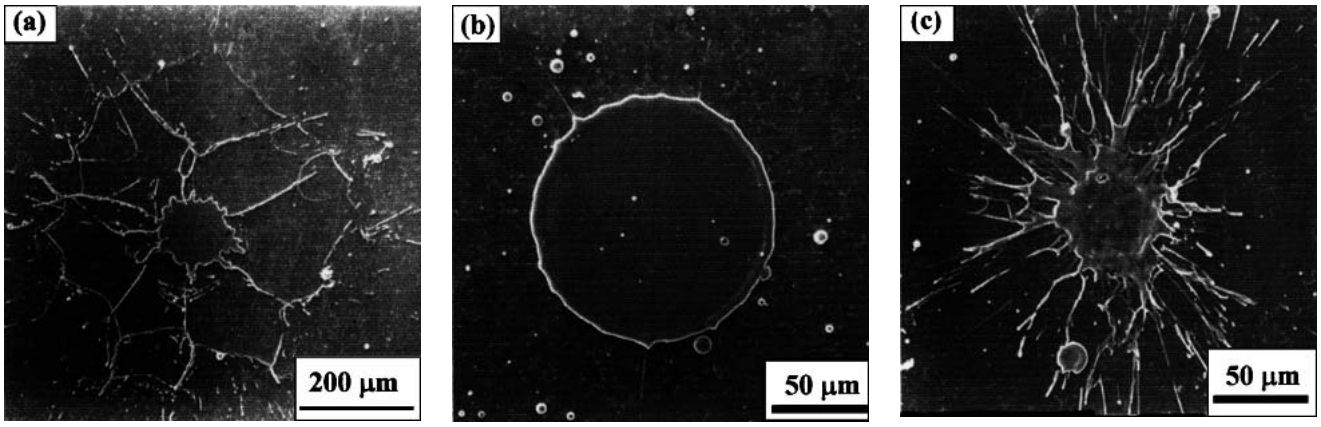


**Fig. 2** Scanning electron micrographs showing a typical splat morphology of cast iron sprayed at different preheat substrate temperatures: **(a)** splash type ($T_S$ = 323 K), **(b)** disk ($T_S$ = 473 K), and **(c)** star shape ($T_S$ = 573 K)

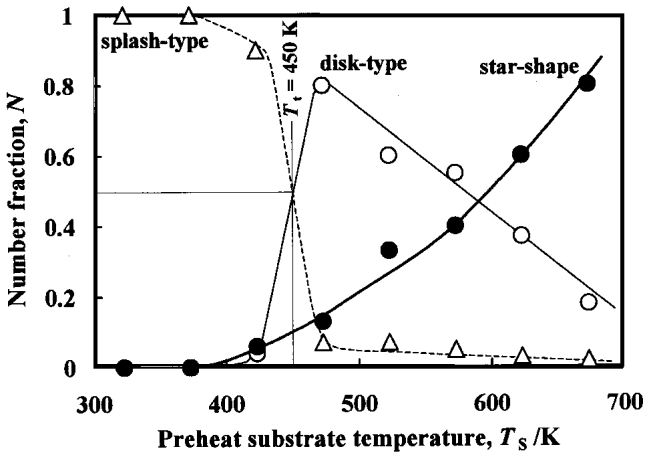


**Fig. 3** Change in splat morphology of sprayed cast iron as a function of preheat substrate temperature

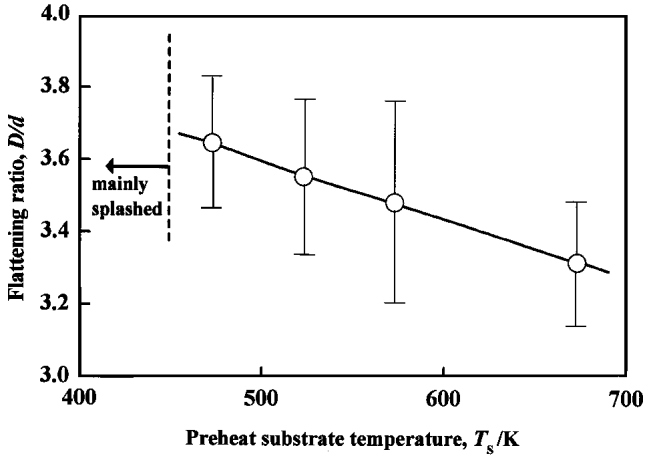


**Fig. 4** Change in flattening ratio of cast iron disk splats as a function of preheat substrate temperature

with substrate temperature, so that they are in the majority above 600 K.

The flattening ratio of splat diameter ($D$) to molten droplet diameter ($d$) was calculated on disk-type splats, as shown in Fig. 4. However, we cannot calculate the flattening ratios below the transition temperature, because the cast iron splats mainly become a splash type. Above the transition temperature, there exists a slight decrease in the flattening ratio with substrate temperature. The preheating slightly develops the oxide layer thickness on a substrate surface, which has been revealed by Auger electron spectroscopy (AES). The oxide layer on a surface preheated at 673 K in a low-pressure argon atmosphere becomes about 1.5-times thicker compared with that on the original surface.

To examine the reason for the decrease in flattening ratio, we observed splat cross sections, as shown in Fig. 5 in the extreme case. Deformed substrate ridges are recognized immediately adjacent to the splat periphery sprayed at high substrate temperatures. These ridges are formed mainly because of the movement of the slightly melted substrate surface upon the impingement of droplets and their expansion. The ridge formation is also supported by EPMA observation, in which the disk-type splat peripheries are surrounded by an oxygen-concentrated region. During the flattening, the kinetic energy of molten droplets is exhausted through friction, which removes the slightly melted layer along with the thin oxide surface. The surface melting is advanced further with an increase in substrate temperature. The ridges restrain the splat expansion on a substrate surface, and consequently the splats decrease in diameter with an increase in substrate temperature.

We then considered the temperature gradient within a flat aluminum alloy substrate impinged by a molten cast iron droplet. The general differential equation for heat conduction is described by Eq 1, for one-dimensional heat flow:

$$dT/dt = (k/\rho C_p)d^2T/dx^2 \quad \text{(Eq 1)}$$

After some solidification has occurred in a splat, the temperature profile in the substrate and the splat is schematically given at the top of Fig. 6, in which we assume the condition of no contact resistance at the splat/substrate interface. The substrate is ini-

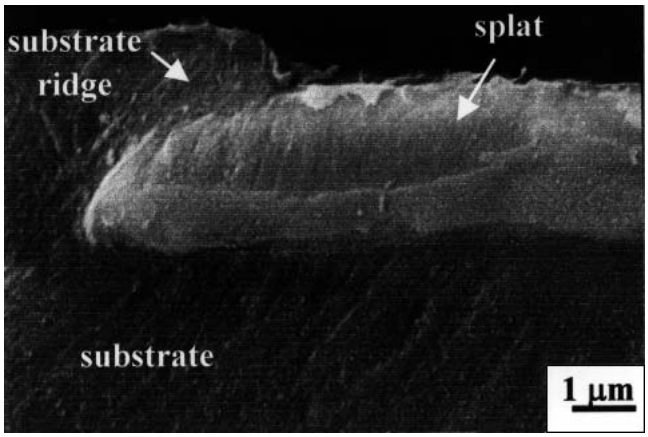


**Fig. 5** Scanning electron micrograph showing a deformed substrate ridge adjacent to the splat periphery ($T_S$ = 473 K)

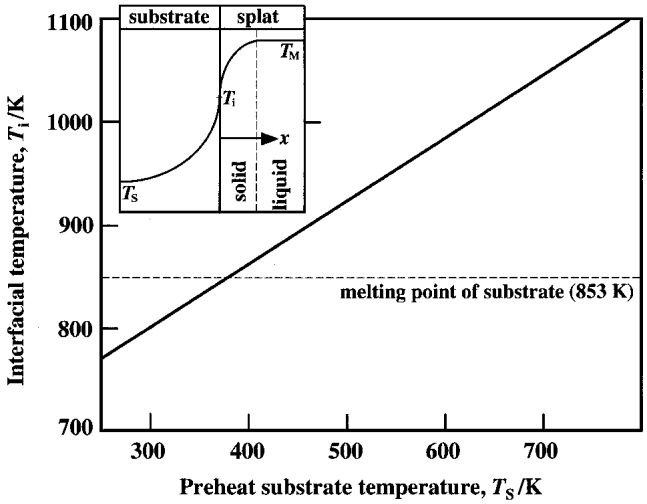


**Fig. 6** Calculated interfacial temperature between splat and substrate without considering the interface resistance

**Table 2 Thermal Properties of Splat and Substrate for the Calculation of Interfacial Temperature**

| | Cast Iron Splat | Al-Si-Cu Substrate |
|---|---|---|
| Thermal conductivity (J/m · K · s) | $k$ = 33 | $k$ = 150 |
| Solid density (kg/m$^3$) | ρ = 7300 | ρ = 2740 |
| Specific heat (J/kg · K) | $C_P$ = 670 | $C_P$ = 1100 |
| Heat of fusion (kJ/kg) | $H_f$ = 201 | … |
| Melting point (K) | $T_M$ = 1423 | $T_{Al}$ = 853 |

tially preheated at a given temperature ($T_S$) and the molten splat is preheated at its melting point ($T_M$) without superheat. The heat flux into the splat/substrate interface from the molten splat must equal the flux away from the interface into the substrate. The substrate is semi-infinite in the negative $x$-domain with the interfacial temperature ($T_i$), which is determined by the thermal properties of both the splat and the substrate, as listed in Table 2. The solution of the temperature distribution within the semi-infinite substrate is given by Eq 2:

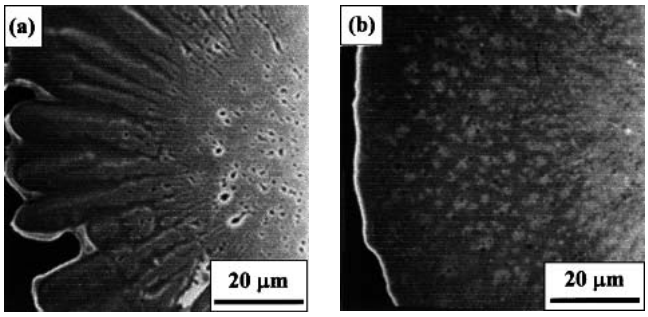


**Fig. 7** Typical rear views of cast iron splats peeled away from a substrate surface: **(a)** splash ($T_S$ = 423 K) and **(b)** disk ($T_S$ = 473 K)

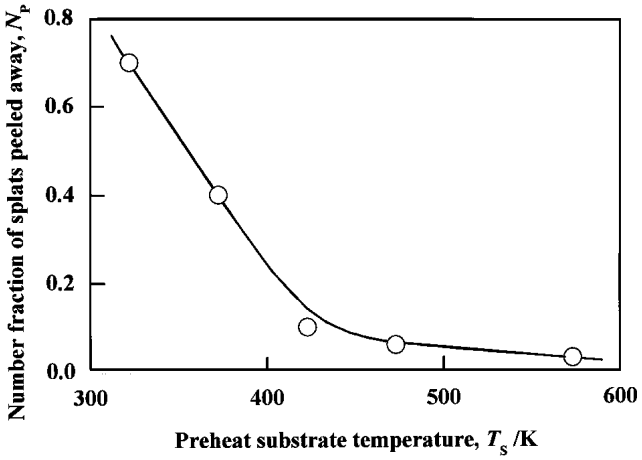


**Fig. 8** Change in number fraction of cast iron splats peeled away as a function of preheat substrate temperature

$$(T - T_i)/(T_S - T_i) = \text{erf}\{-x/[2(kt/\rho C_p)^{1/2}]\} \quad \text{(Eq 2)}$$

According to the Geiger and Poirier's method,[19] $T_i$ is calculated as shown in Fig. 6 with different $T_S$, in which the melting point of the substrate is also described. The interfacial temperature ($T_i$) linearly increases with an increase in $T_S$. The temperature at the substrate surface becomes higher than its melting point for $T_S$ > 380 K. This particular spraying is characterized by an impingement of high melting point droplets onto a low melting point substrate. However, the above consideration does not involve the thermal resistance at the interface, which means the interfacial contact is intimate, containing no pores. Actually, there exist many pores at the interface sprayed with relatively low $T_S$, so that the interfacial temperature becomes lower than the above-calculated values. The pore formation of the thermal resistance will be discussed in the next section.

### 3.2 Formation of Pores and Reaction Layer at the Interface

The rear views of cast iron splats sprayed at substrate temperatures of 423 and 473 K are shown in Fig. 7, in which the splat morphology is a splash type at low substrate temperature (423 K) and a disk type at high temperature (473 K). There exist many

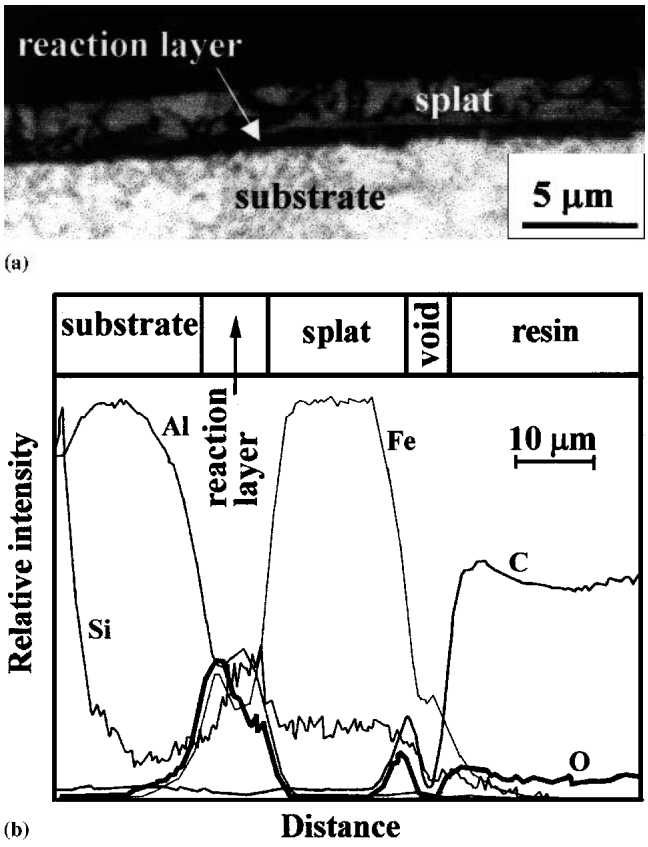


**Fig. 9** Typical reaction layer at the interface between cast iron splat and substrate ($T_S$ = 473 K): **(a)** optical micrograph showing a cross-section microstructure and **(b)** element distribution on the cross section

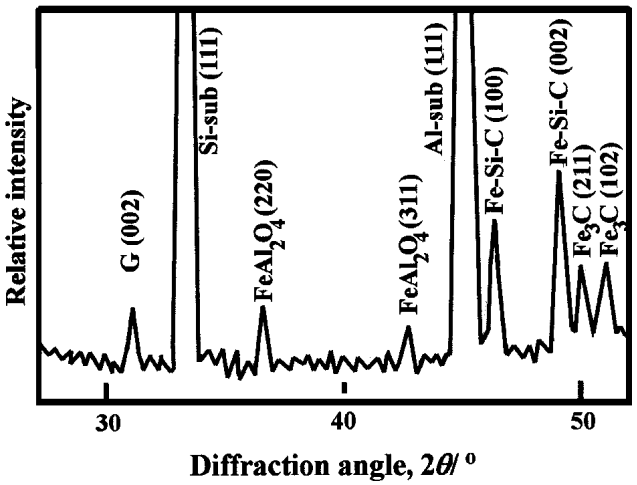


**Fig. 10** Typical x-ray diffraction pattern of cast iron splats sprayed on preheated aluminum alloy substrate ($T_S$ = 473 K)

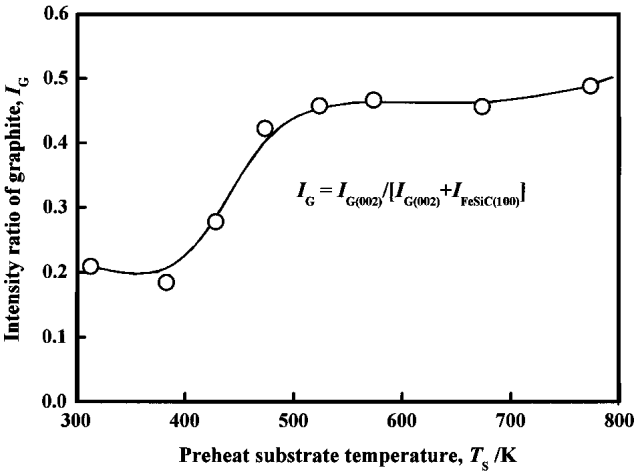


**Fig. 11** Change in intensity ratio of graphite to the sum of graphite and Fe-Si-C on the x-ray diffraction pattern of cast iron splats as a function of preheat substrate temperature

elongated and small pores formed at the interface in the case of splash-type splats shown in Fig. 7(a), so that the adhesive strength of splats seems to be lowered. Elongated pores become wider close to the periphery, but they are not recognized at the splat center. The splat morphology, especially the splashing, is closely related to the elongated pores. The center part of splats makes the first contact against the substrate surface and is subjected to high pressure because of the impingement. Then, the radial force for the expansion strongly acts on the residual molten region to cause splashing. Low friction between a substrate surface and splat arising from pores causes a rapid splat expansion, which causes a splat to splash. On the other hand, the rear view of disk splats is characterized by the formation of very small pores, which leads to relatively good adhesion. It is worth noting that most splats sprayed at high temperatures cannot be removed by an adhesive tape. Furthermore, the pores are mainly generated at the interface from atmospheric and/or absorbed gases on a substrate surface.

The number fraction of splats peeled away decreases with an increase in substrate temperature ($T_S$), as described in Fig. 8, in which the total number of splats has been counted on a substrate before the peeling away. An increase in adhesive strength with substrate temperature approximately coincides with a change in the splat morphology; that is, disk- and star-shaped splats exhibit good adhesive strength. Hence, it is necessary to form highly adhered disk- and star-shaped splats by preheating a substrate for the purpose of improving the adhesive strength of sprayed coatings.

The formation of a reaction layer was examined on the cross-sections, as shown in Fig. 9(a), of an optical micrograph taken on splats sprayed at 473 K. The rather thick reaction layer appears at the interface sprayed above the transition temperature of 450 K. To analyze the chemical composition, element analyses of EPMA have been carried out on the cross section of cast iron splats sprayed at various substrate temperatures, as typically shown in Fig. 9(b) at 473 K. The main components are iron, aluminum, and oxygen in the reaction layer, in which the characteristic x-ray intensity of Si-Kα and C-Kα are not high. The mutual diffusion through the slightly melted substrate surface occurs to form the reaction layer, such as $FeAl_2O_4$, during the solidification on a preheated substrate surface. This, together with deformed substrate ridges, improves the adhesive strength. Thus, it becomes more difficult to peel away the splats sprayed

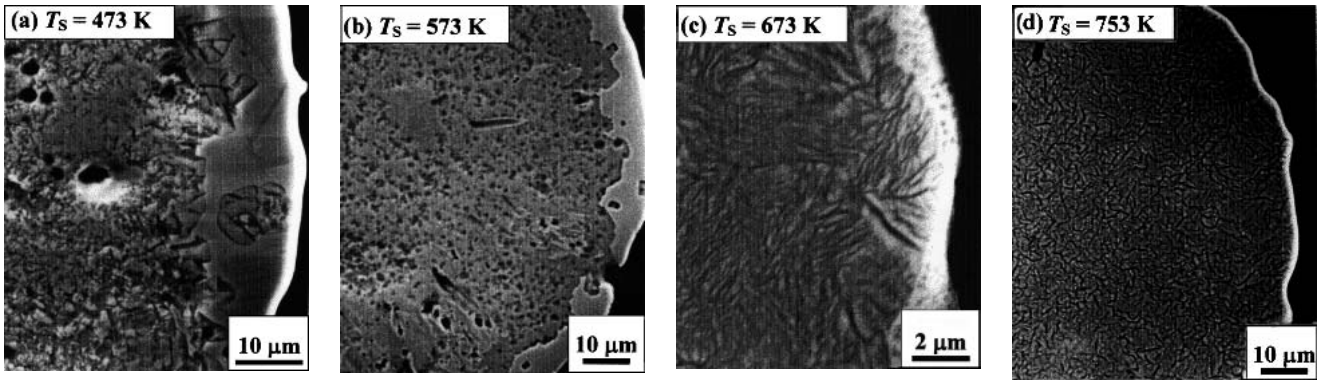


**Fig. 12** Scanning electron micrographs showing a top view of cast iron disk splats sprayed at different substrate temperatures

at high substrate temperatures. In contrast, splash-type splats, which exhibit poor adhesive properties, do not form such an appreciable reaction layer.

### 3.3 Microstructure and Graphite Formation in Splats

A series of XRD patterns has been taken on splats sprayed at different substrate temperatures to study the effect of preheating on the constituent phases, especially the formation of graphitized carbon. The splats are composed of a rapidly solidified phase of Fe-Si-C, $Fe_3C$, graphite, and $FeAl_2O_4$, as typically shown in Fig. 10, sprayed at 473 K. A change in the diffraction intensity ratio of graphite relative to the sum of graphite and Fe-Si-C is shown in Fig. 11 as a function of substrate temperature. The intensity ratio of graphite increases with substrate temperature, but reaches the saturated value above a substrate temperature of 500 K. The solidification rate of cast iron splats depends on preheat substrate temperature and interfacial thermal resistance. At low substrate temperatures, the thermal resistance becomes higher because of pores at the interface, which causes the lowered solidification rate. However, at high substrate temperatures, the simple Newtonian heat conduction analysis[19] reveals the long solidification period, such as the order of 1 μs in the case of a superheat of a cast iron splat; this is also supported by an increase in graphite.

Scanning electron micrographs of a top view of splats sprayed at different substrate temperatures are shown in Fig. 12. The splat microstructures of Fig. 12(a) and (b) are first characterized by $Fe_3C$ at the periphery: the amount of $Fe_3C$ decreases with an increase in substrate temperature, which agrees with the XRD patterns. Below substrate temperatures of 573 K, the splats contain small black areas, the sizes of which decrease with preheating. According to the spot analyses of EPMA with a focused electron beam of about 1 μm in diameter, some of the black areas contain more than 40 wt.% carbon, which are probably graphite. However, the remaining comparatively large black areas contain iron, aluminum, oxygen, and a small amount of carbon, which seems to be the reacted oxide of $FeAl_2O_4$. Features appearing as black lines are resolved above 673 K in place of the black areas (Fig. 12c). The black line microstructure becomes coarser at the higher substrate temperature of Fig. 12(d). When we compare these features with those of splats annealed at 773 K for 3.6 ks in an argon atmosphere, the black line microstructure grows to form graphite. Hence, the splat solidification rate, determined by the splat thickness, reaction layer, and pores, affects the graphite and $Fe_3C$ formation in plasma sprayed cast iron splats on a preheated substrate.

## 4. Conclusions

The effects of preheat substrate temperature on the splat morphology and microstructure of cast iron were examined on a mirror-polished aluminum alloy substrate as a fundamental study on plasma sprayed cast iron coatings. The following results were obtained.

- Preheat substrate temperature greatly affects the splat morphology of cast iron. There exist three different types of splats; that is, splash-type splats appear at low substrate temperatures and both disk- and star-shaped splats appear at high temperatures.
- Deformed substrate ridges, mainly caused by the slight melting of a substrate surface, are formed immediately adjacent to the splat periphery sprayed at high substrate temperatures. The flattening ratio decreases with preheating, because the ridges act as an obstacle to the splat expansion.
- Splash-type splats exhibit poor adhesive properties because the pores appeared at the interface. Small amounts of disk- and star-shaped splats are peeled away, so that they show good adhesion through a reduction in the pore size and the amount.
- The reaction layer composed of iron, aluminum, and oxygen appears at the interface sprayed at high substrate temperatures. The pore formation prevents the reaction layer from developing, which leads to the poor adhesive strength.
- The splats are composed of rapidly solidified Fe-Si-C, $Fe_3C$, graphite, and $FeAl_2O_4$. The formation of graphitized carbon is slightly promoted with an increase in substrate temperature.

### Acknowledgments

The present work was partially supported by the Grants-in-Aid for Scientific Research (12450306) and by the Grants-in-

Aid for Academic Frontier Center from the Ministry of Education, Science, Sports and Culture.

## References


1. M. Ebisawa, T. Hara, T. Hayashi, and H. Ushio: "Production Process of Metal Matrix Composite (MMC) Engine Block," SAE Tech. Paper Series, 910835, 1991.
2. K. Funatani, K. Kurosawa, P.A. Fabiyi, and M.F. Puz: "Improved Engine Performance via Use of Nickel Ceramic Composite Coatings," SAE Tech. Paper Series, 940852, 1994.
3. M.R. Kim and R.W. Smith: "High-Deposition Rate Coating of Aluminum Cylinder Bores" in *Proceedings of the 7th National Thermal Spray Conference,* Boston, MA, 1994.
4. L. Byrnes and M. Kramer: "Method and Apparatus for the Application of Thermal Spray Coatings onto Aluminum Engine Cylinder Bores" in *Proceedings of the 7th National Thermal Spray Conference,* Boston, MA, 1994.
5. G. Wuest, G. Barbezat, and S. Keller: "The Key Advantages of the Plasma-Powder Spray Process for the Thermal Spray Coating of Cylinder Bores in Automotive Industry," SAE Tech. Paper Series, 970016, 1997.
6. A. Rabiei, D.R. Mumm, J.W. Hutchinson, R. Schweinfest, M. Ruhle, and A.G. Evans: "Microstructure, Deformation and Cracking Characteristics of Thermal Spray Ferrous Coatings," *Mater. Sci. Eng.,* 1999, *A269,* pp. 152-65.
7. K. Murakami, T. Okamoto, Y. Miyamoto, and S. Nakazono: "Rapid Solidification and Self-Annealing of Fe-C-Si Alloys by Low Pressure Plasma Spraying," *Mater. Eng. Sci.,* 1989, *A117,* pp. 207-14.
8. R. McPherson: "The Relationship between the Mechanism of Formation, Microstructure and Properties of Plasma Sprayed Coatings," *Thin Solid Films,* 1981, *83,* pp. 297-310.
9. T. Watanabe, I. Kuribayashi, T. Honda, and A. Kanzawa: "Deformation and Solidification of a Droplet on a Cold Substrate," *Chem. Eng. Sci.,* 1992, *47*(12), pp. 3059-65.
10. C.S. Marchi, H. Liu, E.J. Lavernia, R.H. Rangel, A. Sickinger, and E. Muehlberger: "Numerical Analysis of the Deformation and Solidification of a Single Droplet Impinging onto a Flat Substrate," *J. Mater. Sci.,* 1993, *28,* pp. 3313-21.
11. C.C. Berndt, W. Brindley, A.N. Goland, H. Herman, D.L. Houck, K. Jones, R.A. Miller, R. Neiser, W. Riggs, S. Sampath, M. Smith, and P. Spanne: "Current Problems in Plasma Spray Processing," *J. Therm. Spray Technol.,* 1992, *1*(4), pp. 341-56.
12. R.C. Dykhuizen: "Review of Impact and Solidification of Molten Thermal Spray Droplets," *J. Therm. Spray Technol.,* 1994, *3*(4), pp. 351-61.
13. A. Hasui, S. Kitahara, and T. Fukushima: "On Relation between Properties of Coating and Spraying Angle in Plasma Jet Spraying," *Trans. Natl. Res. Inst. Met.,* 1970, *12*(1), pp. 9-20.
14. V.V. Sobolev: "Morphology of Splats of Thermally Sprayed Coatings" in *Thermal Spray Meeting the Challenges of the 21st Century, 1,* C. Coddet, ed., ASM International, Metals Park, OH, 1998, pp. 507-10.
15. M. Fukumoto and Y. Huang: "Flattening Mechanism in Thermal Sprayed Nickel Particles Impinging on Flat Substrate Surface," *J. Thermal Spray Technol.,* 1999, *8*(3), pp. 427-32.
16. M. Fukumoto, S. Katoh, and I. Okane: "Splat Behavior of Plasma Sprayed Particles on Flat Substrate Surface, Thermal Spraying—Current Status and Future Trends," A. Ohmori, ed., *J. High Temp Soc., 1,* 1995, pp. 353-58.
17. C. Moreau, P. Cielo, and M. Lamontagne: "Flattening and Solidification of Thermally Sprayed Particles," *J. Therm. Spray Technol.,* 1992, *1*(4), pp. 317-23.
18. M. Fukumoto, T. Yokoyama, K. Oku, and Y. Tanaka: "Optimization of Substrate Preheating Condition on Adhesive Strength of Thermal Sprayed Coating," *J. High Temp. Soc.,* 1997, *23*(Suppl.), pp. 240-46.
19. G.H. Geiger and D.R. Poirier: *Transport Phenomena in Metallurgy,* Addison-Wesley, Reading, MA, 1973, pp. 329-49.